Realization of a Diffraction-Based 1x100 Optical Switch

Rachel Sampson,[1] Jilian Nguyen,[2] Feibien Cheah,[2] and Pierre-Alexandre Blanche[2]

[1] *Department of Physics and Astronomy, Stony Brook University, Stony Brook, NY 11794-3800, USA*
[2] *The College of Optical Sciences, University of Arizona, Tucson, Arizona 85721, USA*

(Dated: August 19, 2015)

A 1x100 diffraction-based optical switch was designed for use in data centers. The switch decouples the send- and receive-side components, allowing for independent scaling of the two sides, is bandwidth-invariant, and has a rapid reconfiguration time [12 μs]. These properties combine to create a robust technology capable of adapting to the rapidly changing demands of data centers.

In the switch, 1550 nm laser light is shone onto a digital micromirror device (DMD). The DMD acts as an active steering unit and diffracts incident light at precalculated angles using computer generated holograms. The DMD however has a limited angular range, which translates into a restricted spatial span. In order to increase the spatial range of the switch, so that all racks within the data center can be accessed, a mirror assembly is used. Light diffracted off the DMD hits the mirror assembly and is redirected to the desired destination racks. The angles of the mirrors in the mirror assembly are predetermined so that each mirror connects a source rack to one destination rack. The switch was modeled in Zemax, an optical design program, and serves as a proof-of-concept that 1xN diffraction-based optical switches can be created. Future research will focus on further increasing the number of output ports.

I. INTRODUCTION

Data traffic has increased exponentially in recent years with annual international internet traffic and bandwidth increasing by 40% over the past four years. This trend is predicted to continue with forcasts anticipating a threefold increase in data traffic between 2014 and 2019 [1]. This rapid increase in traffic is a driving force behind data center's changing bandwidth and power demands. Given the quickly changing landscape of modern telecommunications, it is imperative that future designs for telecommunication technology are dynamic, flexible, and efficient to keep up with the changing demands.

At the start, telecommunications made use of electrical signals to transmit information. However, a shift to optical fibers occurred because of fiber's large bandwidth and the ease of multiplexing signals [2]. Optical fibers are now used by many data communication networks [2].

Switches are devices which route information; in instances where the signal is being transmitted optically, switches connect different fibers [3]. In the past, the switches that connected optical fibers involved both optical and electrical elements. Data was transferred optically, manipulated electrically, then finally transmitted optically [3]. This process acted as a bandwidth bottleneck, was slow, required rigid infrastructures, and had high energy costs [2]. Many novel solutions have been proposed in recent years to improve upon the traditional switch [4–11]. One line of research has focused on the development of all optical switches to streamline the switching process [2–4, 12, 13].

Optical switches have the advantage, over optical-electrical switches, of being highly robust and efficient [12]. The performance of an optical switch is independent of bandwidth or protocol allowing them to be resilient to future increases in bandwidth, unlike electrical switches which experience a "fall off" as a function of frequency, and new controlling and multiplexing algorithms [12]. Optical switches also do away with much of the cabling necessary for modern-day switches. Their simpler architecture allows the optical switches to be more easily reconfigured to update their capabilities. With the hastily changing traffic flow, being able to easily and quickly update one's system is essential. All of these properties combine to create a dynamic and flexible technology, which is capable of handling the rapidly changing demands of modern-day telecommunications.

The goal of this project was to construct a diffraction-based, non-blocking 1xN optical switch using a digital micromirror device (DMD). DMD based optical switches are advantageous due to their very high port count, moderate loss, μs reconfiguration times, low power consumption, and high reliability. The diffraction-based switch we have designed also has the advantage of being easily reconfigured and decoupling the send- and transmit-components of the switch. The ultimate goal of this research is to create a 1xN optical switch where N is on the order of 10,000 for use in data centers. This paper describes the design of a 1x100 optical switch that was designed as a proof-of-concept. Future research will focus on increasing the number of output ports.

Designing an 1xN diffraction-based optical switch entailed modeling and optimizing the system in Zemax, an optical design program. In the system, computer generated holograms (CGHs) uploaded onto a DMD are used for fine control of the angular output of diffracted beams. The DMD had a limited angular range of 3^o. To increase the spatial span of our switch, mirror assemblies were positioned on the ceiling of the data center above each rack to redirect the diffracted beams to their intended destination racks. Two mirror angles were calculated for each mirror in the mirror assembly, so that the beam could be redirected in both the x- and y-direction. The methods and results of our calculations are detailed in

the following sections.

II. OPTICAL SWITCH OVERVIEW

The switch we designed for use in data centers is pictured in Fig.1. Lasers placed on the top of the racks within the data center shine on to DMDs which use precalculated CGHs to diffract the light into a predetermined pattern. The DMD in our set-up suffers the limitation of having a limited angular range of 3^o. This very limited angular range severely limits the spatial reach of light which is diffracted off of the DMD.

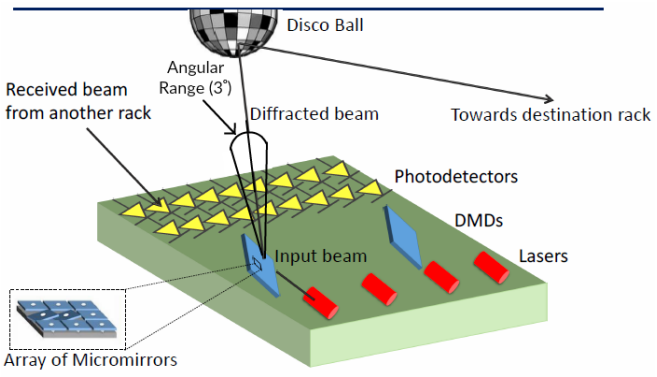

FIG. 1: Top of rack with 1xN optical switch configuration

To increase the spatial reach of the DMD, a mirror assembly placed on the ceiling of the data center is used. There will be one mirror assembly above each rack. The mirror assembly consists of an array of static micromirrors positioned in such a way that light incident on it will be redirected to one of the possible destination racks.

For this project, we modeled the data center as a series of equally spaced data racks. The racks were arranged in a 10 x 10 configuration with a separation of 1.1 m between racks. This is similar to the spacing between racks in an actual data center. A schematic of our set-up is shown in Fig. 2. The rack (5,5) was chosen as the source for which we designed our mirror assembly.

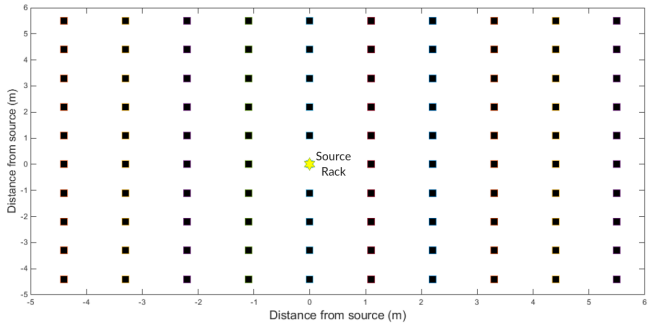

FIG. 2: Schematic of data center configuration

Each of the racks will also have an array of detectors on top of it, which will detect incident light. We propose using photodetectors, which are cheap and plentiful, and operate by either detecting a 1 or 0 depending on whether the incident light passes a power threshold.

The optical switch we designed, as shown in Fig. 3, is composed of lenses, a Texas Instrument DLP 7000, and a redirecting mirror assembly. The DMD acts as a beam steering device, while the mirror assembly effectively increases the spatial range of the DMD. The set-up described below was designed for the near infrared ($\lambda = 1550$ nm). Experimental testing will begin with a visible light set-up ($\lambda = 532$ nm). Below, we describe in detail how the parameters of each optical element were chosen.

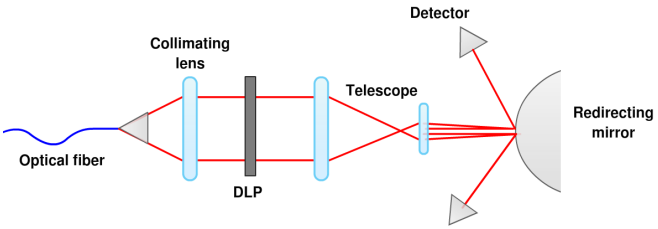

FIG. 3: 1xN optical switch configuration

A. Collimating Lens

The first lens in our system served to collimate the beam and was chosen such that the output beam's diameter was equal to the clear aperture of the DLP. The focal length and clear aperture of the lens were chosen to meet this criteria.

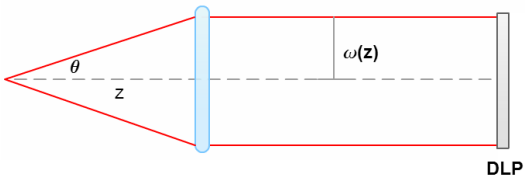

FIG. 4: Ray diagram of the first leg of the set up

To determine the focal length of the lens needed, we first found the divergence of the beam leaving the single mode fiber, using the equation:

$$\theta = \frac{\omega(z)}{z}, \tag{1}$$

where θ is the divergence, $\omega(z)$ is the radius of the beam at a given axial value, and z is the axial distance from

the beam's waist. We found the divergence to be 5.401^o, or 94.3 mrad.

In this case, where we are well outside the Rayleigh range, geometric optics is sufficiently precise to determine the axial distance from the point source at which the beam radius is equal to the DLP's radius. Using Eq.1, we found z equal to 55.56 mm when the beam and the DLP radii are equivalent. To collimate the beam, we must place the lens a focal length away from the object. The reasoning behind this is evident when looking at the lens equation:

$$\frac{1}{f} = \frac{1}{d_o} + \frac{1}{d_i}, \tag{2}$$

where f is the focal length, d_o is the distance to object, and d_i is the distance to image. When d_o=f, then d_i must go to infinity meaning the beam never converges to an image and the beam is collimated.

The Edmund Optics #84-256 lens was chosen to act as the collimating lens in our system. The lens has a 25 mm diameter and a focal length of 53.61 mm. This does not perfectly match the z calculated above, but is sufficiently close and just means that our collimated beam will be slightly smaller in diameter than our DLP.

In Zemax, axial position is defined as the distance to the principal plane of the lens, rather than the first surface. Therefore, to correct for this, and find the correct axial position for the lens, we had to subtract the distance to the principal plane from the focal length.

To determine the location of the principal plane of our lens, we used the following equations:

$$d = \frac{\phi_2}{\phi}\tau \quad and \quad d' = \frac{\phi_1}{\phi}\tau \tag{3}$$

where d is the distance from the front surface to the front principal plane, d' is the distance from the back surface to the back principal plane, ϕ_1 and ϕ_2 are the index of refraction minus 1 divided by the opposite surface's curvature, while ϕ is equal to $\phi_2 - \phi_1 + \frac{\phi_1\phi_2}{(n-1)}\tau$, and $\tau = \frac{t}{n}$, where t is the thickness of the lens and n is the index of refraction.

Since we are using a plano-convex lens, the radius of curvature of the first surface is infinity making d'=0 and $d = \frac{t}{n}$. For the lens we selected, $t = 4.9mm$ and $n = 1.5006$, therefore d is equal to 3.27 mm and the lens should be placed at z=50.35 mm.

B. Digital Micromirror Device

Once the light is collimated by the first lens, it's then incident on a DMD. A Texas Instruments Digital Light Processor (DLP) 7000 was used as the DMD in this set-up. The DLP consists of 1024x768 micro-mirror array with a pixel pitch of 13.68 μm. Each of the mirrors can be oriented at $\pm$ 12^o. The incident light either sees the pixel as ON or OFF depending on the orientation of the mirror.

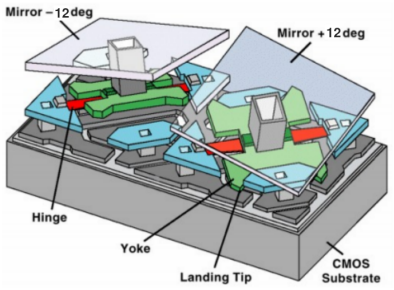

FIG. 5: Close-up of mirrors in DMD
Image courtesy of Texas Instruments

To determine the angular range of the DMD, the diffraction grating equation was used:

$$sin(\theta_i) + sin(\theta_d) = \frac{m\lambda}{d}, \tag{4}$$

where θ_i is the angle of incidence, θ_d is the diffracted angle, m is the diffraction order, λ is the wavelength, and d is the grating line width. The maximum amount of light is diffracted into the first order when the light incident on the DLP is at an angle of 14^o with respect to the x-axis and 0^o with respect to y-axis [2].

The largest angle at which light will be diffracted off the DLP will correspond to when the Bragg condition is met. The smallest diffraction angle will correspond to when d is equal to the width of active area of the DLP. Using Eq. 4, a diffracted angle with respect to the x-and to the y-axis was calculated for both conditions. This yielded a minimum angle of -10.68^o and a maximum angle of -13.99^o with respect to the x-axis. This means the angular range with respect to the x-axis was 3.31^o. With respect to the y-axis, the diffracted angle varied from 3.25^o to 0.01^o yielding a range of 3.24^o. These represent the range of angles at which light can be diffracted from the DLP.

C. Telescope

After the light diffracts off of the DMD, it passes through a Keplerian telescope, as pictured in Fig.6. The Keplerian telescope in this set-up serves two purposes: 1) it allows for spatial filtering at the focal plane of the first lens to separate the first diffraction order and 2) it down-collimates the beam so that the beam fits on the mirrors of the mirror assembly. In order to achieve this, a very long and short focal length lens are needed.

The lateral and angular magnification of our Keplerian telescope is given by:

$$M = \frac{-f_2}{f_1} = \frac{h_i}{h_o}, \tag{5}$$

where m is the magnification of the telescope, f_1 is the focal length of the first lens, f_2 is the focal length of the second lens, h_o is the radius of the input beam, and h_i is the radius of the output beam.

In order to ensure the profile of the beam at the output of the telescope highly resembles the image at the focal plane, the magnification of the system must be much less than 1. To achieve this and minimize aberrations from the lenses, two plano-convex lenses with a magnification ratio of 0.2 were used. It was experimentally verified that the beam profile at the output of the telescope with this magnification closely resembled the beam at focal plane.

The spatial range of the diffracted beams after the telescope will place an upper limit on the dimensions of our mirror assembly. The size of the beams after the telescope will place a limit on the size of the mirrors. since the angular and lateral magnification of our telescope is 0.2, this means that the angular range of and the size of the diffracted beams should be reduced by a factor of five.

The size of the diffracted beams going into the telescope should be 10.14 mm in diameter, therefore at the output of the telescope, we would expect the beams to be 2.03 mm in diameter. Whereas entering the telescope the angular range of the diffracted beams is 3.31^o in the x-direction and 3.24^o in the y-direction, out of the telescope it's 0.62^o in the x-direction and 0.65^o in the y-direction. The beam diameter and angular range of the beams coming out of the telescope place a lower limit on the mirror size on the mirror assembly and an upper limit on the mirror assembly size.

D. Mirror Assembly

After the diffracted beams leave the telescope, they will be incident in a mirror assembly. Our 1x100 optical switch will include an assembly of 100 mirrors, which will be used to redirect the light diffracted off of the DLP into the desired output port. We plan on designing the mirror assembly in Solidworks, a computer-aided design program, and then exporting the design to Zemax. We then hope to have the piece machined using a Moore Nanotech 350FG Ultra-Precision Freeform Generator, a CNC diamond turning machine.

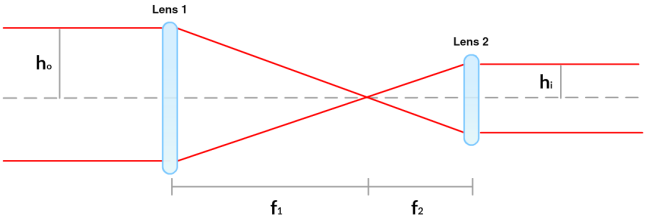

FIG. 6: Schematic of a Keplerian telescope

The resolution and travel of the diamond turning machine will place constraints on the size of the individual mirrors and the assembly as a whole. The straightness in the critical direction resolution in the x, y, and z axes is 300 μm making the lower constraint on the size of our mirrors 300 μm. The machine has a travel of 350, 150, and 300 mm in the x, y, and z axes respectively, therefore our assembly cannot exceed these dimensions. The travel places an upper limit on our mirror size of approximately 30 x 30 mm.

The beam size and angular range of the diffracted beams after the telescope will act as the limiting constraints on the mirrors' size and the mirror assembly. The dimensions of the mirrors must be larger than the diameter of the beam to ensure the beams fully fit on the mirrors. The mirrors will be rectangular shape due to the packing configuration chosen, as discussed in the next section, with the length being twice the width. The width must be at least 2.027 mm and the dimensions of the mirror assembly must be at maximum 4.4 cm by 4.3 cm. We therefore choose to make the mirrors 2.1 by 4.2 mm in size.

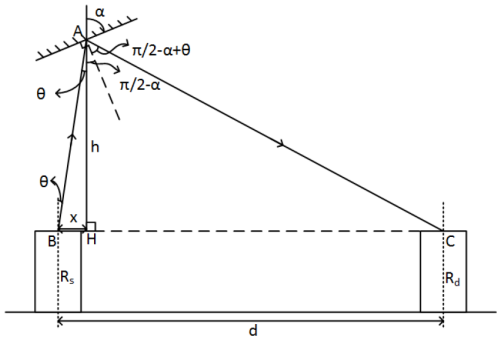

FIG. 7: Schematic of optical switch set-up

Fig.7 shows a cross-section of the optical switch set-up. To determine the angle at which each mirror in the assembly should be placed in order for the source to communicate with the intended destination rack, the following equation was used:

$$\alpha = 90 - 0.5\left[\pi + \theta - tan^{-1}\left(\frac{h - dtan\theta}{h}\right)\right], \tag{6}$$

where θ is the angle with respect to normal at which light leaves the rack, h is the distance between the top of the rack (ToR) and the ceiling, d is the height of the rack, and α is the angle at which the mirror should be oriented with respect to the ceiling. Here, d was set to 2.2 m and h was set to 3.8 m to match the usual parameters of a data center. A mirror angle was calculated with respect

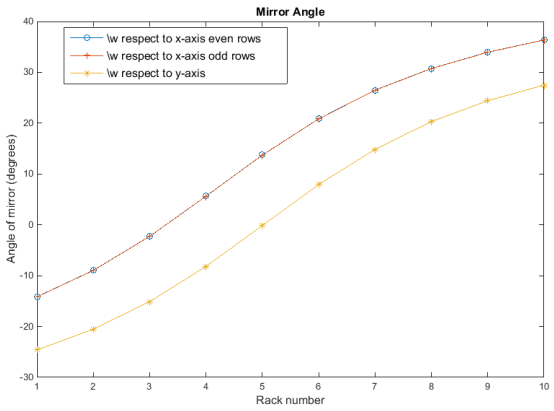

FIG. 8: Angle at which mirror is oriented with respect to the ceiling with respect to the x- and y-axis. The two plots with respect to x-axis are due to adjacent rows in the mirror assembly having a translational offset.

to both the x- and y-axis. Fig. 8 shows the results of these calculations.

As is seen in Fig. 8, the angle at which the mirror was positioned ranged from -10^o to 40^o with respect to the x-axis and from approximately -20^o to 30^o. The angle curve is asymmetric because the rack (5,5) was chosen as the source rack out of an array of 10 by 10 racks, so the problem is not symmetric.

III. NUMBER OF ACCESSIBLE LOCATIONS

An important parameter of our switch is how many output ports it can reach. Due to the Fourier transform relation between a hologram and its image, the number of pixels on the DMD will be equivalent to the number of possible diffracted beam locations. In order to maintain distinct beams though, only some of locations accessible by the DLP can be utilized. Only locations with sufficiently low crosstalk can be used. Crosstalk occurs when signal intended for one detector is measured at another undesired detector. In optical communications, crosstalk below -40 dB is generally demanded for a sufficiently low signal to noise ratio for efficient data transfer [13]. We sought to determine what configuration would yield the greatest number of accessible locations while respecting the -40dB cross talk criteria. We modeled a square lattice as reference and a parallelogram lattice.

In the square lattice, all four sides of the unit area are equivalent and the sides are perpendicular to one another. In the parallelogram lattice, there existed two pairs of equivalent length sides and the angles kitty corner to each other were equivalent. The two configurations are shown in Fig.9.

We started by determining the distance at which two adjacent beams would have to be separated for the cross talk to meet the -40dB threshold. We found the threshold was met when the beams were separated by approximately 2.7 beam radii.

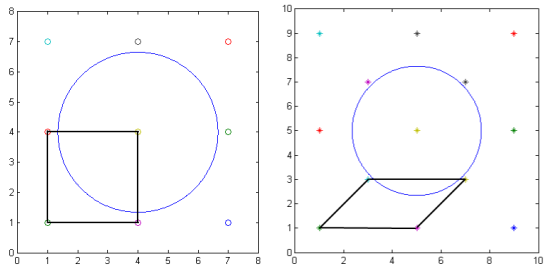

(a) Square (b) Parallelogram

FIG. 9: Matlab model of packing configurations

An analytic solution for the packing factor of each configuration was found. We defined the packing factor as the units of area per point. For the square grid, the packing factor equation was found to be:

$$PF = \frac{9(c-1)(r-1)}{cr}, \tag{7}$$

where c is the number of points in a column, and r is the number of points in a row. For a square configuration, the packing factor converges to 9 units of area per point.

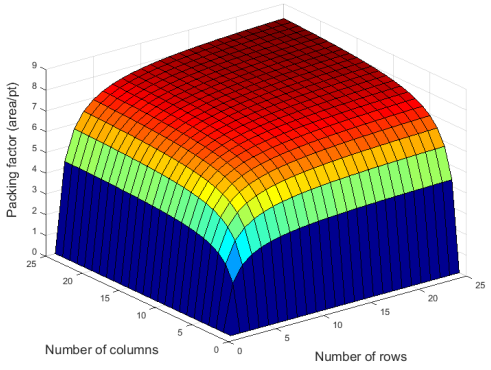

FIG. 10: Packing factor of the square configuration as a function of number of points in a row and column

The analytic solution for the parallelogram configuration for a unit area larger than 5 is as follows:

$$PF = \frac{16(c-1)(r-1)}{5+3(c-2)+3(r-2)+2(c-2)(r-2)}, \tag{8}$$

This configuration converges to 8 units of area per point. This means that the parallelogram lattice has a 1/9th tighter packing factor or can fit 12.5% more points in the same area.

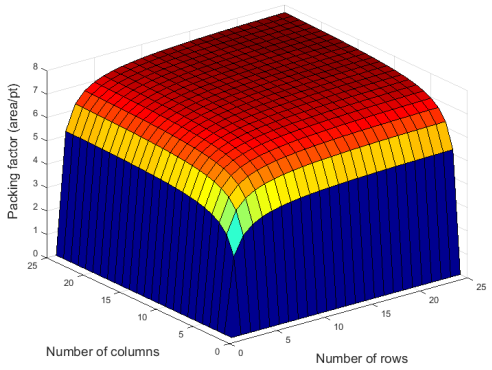

FIG. 11: Packing factor of the parallelogram configuration as a function of number of points in a row and column

The ratio of usable points of the parallelogram versus the square lattice converges to $\frac{9}{8}$. For our 1024 x 768 pixel DLP, the usable number of points was numerically simulated in Matlab and found to be 43,947 points for the square configuration and 49,376 points for the parallelogram configuration. This represents a sizable increase in the number of output points accessible using the parallelogram versus the square output configuration.

Using the parallelogram packing configuration means the beams coming off of the DLP will be arranged in a parallelogram configuration. The mirror assembly will have to be designed in such a manner that each beam hits the center of one of the micromirrors. This can be accomplished by having adjacent rows in the mirror assembly be offset by half a mirror length. iven the configurations dimensions and having the mirrors length be twice as great as their width.

IV. CONCLUSIONS

The preliminary design for a 1x100 diffraction-based optical switch has been reviewed. The switch makes use of a DMD for beam steering, and a mirror assembly to increase the spatial reach of the optical switch. Optical components were chosen or designed for all sections of the optical switch. The mirror assembly still needs to be designed in Solidworks, and machined before the design can be tested experimentally. It was determined that a parallelogram packing configuration yields the greatest number of accessible points, increasing the number of accessible points by 12.4%.

Future work will aim to experimentally verify the theoretical model described herewithin and increase the number of output ports. The current design was also optimized for a single diffracted beam; we hope to more accurately model the system by optimizing the system for multiple diffracted beams.

V. ACKNOWLEDGMENTS

This work was conducted with the support of CIAN NSF ERC under grant #EEC-0812072 and NSF grant #CHE-1156598. The authors would also like to acknowledge the support of Texas Instruments. Lastly, many thanks to Colton Bigler, Brittany Lynn, and Alexander Miles for their helpful discussion.

VI. BIBLIOGRAPHY

[1] Cisco Visual Networking. Cisco Global Cloud Index: Forecast and Methodology, 2012-2017, (White Paper), Cisco, 2013 (16 June 2014).

[2] P.-A. Blanche; D. Carothers; J. Wissinger; N. Peyghambarian. SPIE Journal of Micro/Nanolithography, MEMS, and MOEMS (JM3), 13 (1), 01110 (2013).

[3] P. -A. Blanche."Fast Optical Switch for Data Communication Applications". Presentation.

[4] N. Hamedazimi; Z. Qazi; H. Gupta; V. Sekar; S. R. Das; J. P. Longtin; H. Shah; and A. Tanwer. Sigcomm 2014, 14, pp. 319330.

[5] N. Farrington *et al.*. Sigcomm 2010, pp. 339350.

[6] G. Porter *et al.*. Sigcomm 2013, pp. 447458.

[7] H. Liu *et al.*. NSDI 2014, pp. 115.

[8] G. Wang *et al.*. Sigcomm 2010, pp. 327338.

[9] A. Singla; A. Singh; and Y. Chen. NSDI12, pp. 239252.

[10] X. Zhou *et al.*. Sigcomm 2012, pp. 443454.

[11] S. Kandula; J. Padhye; and P. Bahl. HotNets 2009.

[12] A. Miles; B. Lynn; P.-A. Blanche; J. Wissinger; D. Carothers; L. LaComb Jr.; R.A. Norwood; N. Peyghambarian. Optics Communications, vol. 334, pp 41-45, (2015).

[13] B. Lynn & P.-A. Blanche,"ProjecToR: Rapidly reconfigurable data center interconnect", unpublished.